

A Study of the Branching Ratio of $H \rightarrow c\bar{c}$ at a Future e^+e^- Linear Collider

Yu, Geum Bong*† and Kang, JooSang

Department of Physics, Korea University, Seoul, Korea, 136-701

Miyamoto, Akiya

KEK, 1-1 Oho, Tsukuba-Shi, Ibaraki-Ken, Japan, 305-0801

Park, Hwanbae

Department of Physics, Kyungpook National University, Taegu, Korea, 702-701

(Dated: January 29, 2020)

We carried out a feasibility study on the measurement of the branching ratio of $H \rightarrow c\bar{c}$ at a future e^+e^- linear collider. We used the topological vertex reconstruction algorithm for accumulating secondary vertex information and the neural network for optimizing c quark selection. With an assumption of a light Higgs mass of $120 \text{ GeV}/c^2$, we estimated the statistical error of $\text{Br}(H \rightarrow c\bar{c})$ to be 20.1% or 25.7% depending on the number of vertex detector layers at the center-of-mass energy of 250 GeV and the integrated luminosity of 500 fb^{-1} .

PACS numbers: 11.15.Ex, 11.30.Qc, 14.65.Dw, 14.80.Bn

I. INTRODUCTION

In the theory of elementary particles, the Higgs boson is introduced to elucidate the origin of particle masses. A single Higgs doublet is introduced in the Standard Model (SM) [1], which gives rise to one scalar particle. Meanwhile other Supersymmetric extended models introduce two Higgs doublets to give vacuum expectation value to up-type and down-type quarks, separately. These models predict not only more than one scalar Higgs boson but also different fermion couplings from those of the SM. A precise measurement of Higgs couplings to fermion will be indispensable to unveil physics of the Higgs sector. According to the global fit to the precision electroweak data [2], the mass of the Higgs boson is between $114.4 \text{ GeV}/c^2$ and $211 \text{ GeV}/c^2$ at 95% C.L. in the case of the SM. In the Minimal Supersymmetric Standard Model [3], a mass of the lightest Higgs boson is estimated to be less than about $130 \text{ GeV}/c^2$ [4]. The precise study of such light Higgs boson is an important physics target at a future e^+e^- linear collider. Even though the $H \rightarrow b\bar{b}$ is dominant for Higgs mass below $140 \text{ GeV}/c^2$, a measurement of the branching ratio of $H \rightarrow c\bar{c}$ at the future e^+e^- linear collider provides an unique opportunity to study Higgs to up-type quark coupling.

Experimentally, a high efficient charm quark identification at the future e^+e^- linear collider is possible only with a high performance vertex detector, of which development is one of the major topics on detector development for the linear collider [5]. To this end, understanding of the detector performance to physics is essentially

important.

In this paper, we show that a measurement of $H \rightarrow c\bar{c}$ is possible at the future e^+e^- linear collider, and its significance depends on the vertex detector performance.

II. HIGGS SIMULATION

In this study, we consider the SM Higgs boson with its mass of $120 \text{ GeV}/c^2$. The center-of-mass energy of 250 GeV is assumed because the production cross-section of Higgs at this energy is 226 fb , which is very close to the highest. We have also concerned about the integrated luminosity of 500 fb^{-1} which corresponds to a few years run of the future e^+e^- linear collider experiment. The event was generated using Pythia 5.7 [6] and only Higgsstrahlung process($e^+e^- \rightarrow Z^* \rightarrow Z^\circ H$) is considered. The branching ratios of the SM Higgs boson are calculated by HDecay program [7]. Depending on the decay modes of Z° , the event topologies are categorized to 4-jet mode($Z^\circ \rightarrow 2\text{-jet}$ and $H \rightarrow 2\text{-jet}$), 2-jet mode($Z^\circ \rightarrow \text{neutrino pair}$ and $H \rightarrow 2\text{-jet}$), and lepton pair mode($Z^\circ \rightarrow \text{charged lepton-pair}$ and $H \rightarrow 2\text{-jet}$). Because our signal is Higgs to $c\bar{c}$ decay mode whose branching ratio is so small($\sim 3\%$), we concentrated on only 2-jet and 4-jet modes. In the case of charged lepton-pair mode, it does not have enough events to study $c\bar{c}$ measurement. As background processes, we considered W^+W^- , $Z^\circ Z^\circ$, and $q\bar{q}$ events whose cross-sections are 15460 fb , 1250 fb , and 47300 fb , respectively.

Events were simulated using fast parametrized simulator [8], which was implemented in the Joint Linear Collider(JLC, recently the name is changed as Global Linear Collider) detector [9]. In this simulator, five parameters of the helical track and their error matrices including non-diagonal elements are generated, thus the quality of the vertices is similar to that of a full simula-

*Current address: Department of Physics and Astronomy, Rochester, New York, U.S.A, NY 14627.

†Corresponding author: gbyu@fnal.gov

number of CCD layers	Beam pipe	1st	2nd	3rd	4th	5th
4	2.0	2.4	3.6	4.8	6.0	
5	1.0	1.2	2.4	3.6	4.8	6.0

TABLE I: The vertex detector options. The radius of beam pipe(in cm), the number of CCD layers of the vertex detector and their positions(in cm) from the center of the beam pipe are listed.

tion. The JLC vertex detector is equipped with four layers of Charge Coupled Device(CCD) at the radius from 2.4 cm to 6 cm, whose intrinsic spatial resolutions are 4 μm in $r\phi$ and z directions. The solenoidal magnet field of the detector is 3 tesla. With a vertex detector constraint, the impact parameter resolution in xy plane($\sigma_{r\phi}$) is $\sqrt{(25/\text{psin}^{2/3}\theta)^2 + 4^2} \mu\text{m}$ and the momentum resolution for charged track($\frac{\Delta p_t}{p_t}$) is $\sqrt{(1 \times 10^{-4}p_t)^2 + 10^{-3}}$. To investigate the influence of the detector parameter on the physics result, we also considered parameter sets with five layers of the vertex detector as shown in the Table I.

In the event reconstruction, jets were reconstructed using JADE clustering algorithm and the vertices were reconstructed using the topological vertex reconstruction algorithm(ZVTOP program) [10]. Based on kinematical variables and reconstructed vertex information, neural network(NN) [11] was formed to identify $H \rightarrow c\bar{c}$ events more efficiently.

We considered the non- $c\bar{c}$ Higgs decays ($H \rightarrow b\bar{b}$, gg , WW^* ; Higgs background) and other processes from e^+e^- collision ($e^+e^- \rightarrow Z^0Z^0$, W^+W^- , $q\bar{q}$; non-Higgs background) as backgrounds of $H \rightarrow c\bar{c}$ measurement.

III. SELECTION OF $H \rightarrow c\bar{c}$

A. 2-jet mode

In 2-jet event study, we clustered particles into 2 jets by adjusting the y_{cut} value of the JADE clustering algorithm(forced 2-jet clustering). The following selection criteria were applied for reduction of backgrounds from e^+e^- collision: (1) the visible energy is between 110 GeV and 143 GeV, (2) the missing transverse momentum between 25 GeV/c and 70 GeV/c , (3) the Higgs mass between 105 GeV/c^2 and 125 GeV/c^2 , (4) the recoil Z^0 mass between 82 GeV/c^2 and 120 GeV/c^2 , (5) thrust between 0.75 and 0.99, (6) Ymax between 0.72 and 0.84, and (7) the mass of each jet between 2 GeV/c^2 and 40 GeV/c^2 . Here the Higgs mass is calculated as an invariant mass of all observed particles and the recoil Z^0 mass is calculated disregarding the initial state radiation. Ymax is the maximum y_{cut} value in JADE clustering algorithm to cluster particle into 2 jets. We also required a successful secondary vertex reconstruction and at least one P_t corrected invariant mass(MSPTM,

$\sqrt{M^2_{\text{VTX}} + |P_t|^2} + |P_t|$) of the secondary vertex be between 0.1 GeV/c^2 and 7.0 GeV/c^2 . Here, the P_t is the total transverse momentum of the secondary tracks with respect to the flight direction of the vertex.

In Fig. 1, we compared the visible energy and Ymax distributions of the signal with the non-Higgs background processes, and the separations are clearly seen in this figure. On the other hand, Higgs background processes have the same kinematic distributions as the signal.

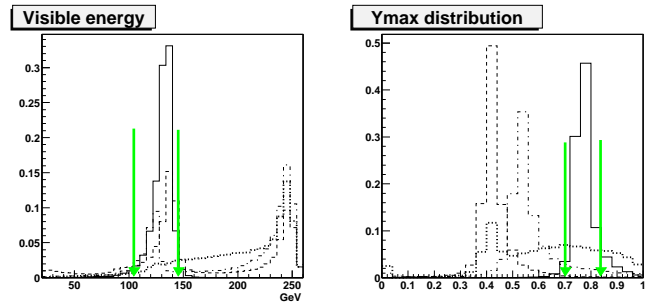


FIG. 1: Cut points of visible energy and Ymax distributions. (solid: Z^0H , dotted: W^+W^- , dash-dotted: Z^0Z^0 , dashed: $q\bar{q}$).

After applying these selection criteria, we trained the NN to maximize the selection quality. We made two sets of training, one against non-Higgs backgrounds, Z^0Z^0 and W^+W^- (Background NN-training), and the other against Higgs backgrounds, $H \rightarrow b\bar{b}$ and gg decays(Higgs NN-training). In the case of $H \rightarrow WW^*$ events, they showed featureless patterns which didn't help NN to separate $c\bar{c}$ patterns from other Higgs decays, and only few $e^+e^- \rightarrow q\bar{q}$ events are remained after the event selection cuts. So we didn't use these events in NN-training although we considered the $H \rightarrow WW^*$ as Higgs background and $e^+e^- \rightarrow q\bar{q}$ as non-Higgs background in $H \rightarrow c\bar{c}$ selection. Normalized input patterns used for the trainings come from the ZVTOP program, which consist of the number of vertices, MSPTM, transverse momentum of the secondary vertex, decay length, invariant mass of the secondary vertex, number of tracks in the secondary vertex, and momentum of the secondary vertex divided by total momentum(corrected secondary momentum). The typical input patterns for Higgs NN-training and Background NN-training are shown in Fig. 2 and Fig. 3, respectively. In particular, for the input patterns of Background NN-training in this 2-jet mode, we used Ymax and jet decay angle in addition to the vertex information.

Using both NN-results of Higgs NN-training and Background NN-training, we made 2D plot and evaluated signal region which gives the best significance. The signal box for $c\bar{c}$ measurement is shown in the right top corner of the Fig. 4.

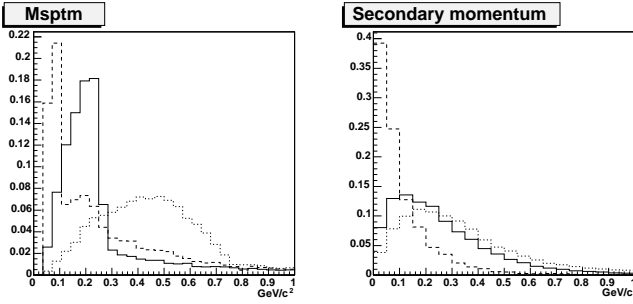


FIG. 2: MSPTM and the corrected secondary momentum distributions as input patterns for $H \rightarrow c\bar{c}$ distinction from Higgs backgrounds. (solid: $H \rightarrow c\bar{c}$, dotted: $bb\bar{b}$, dashed: gg).

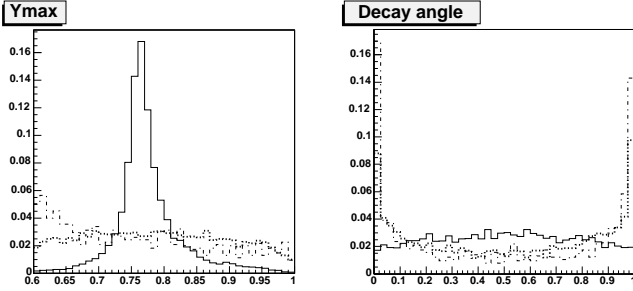


FIG. 3: Ymax and decay angle distributions show good separation between $c\bar{c}$ and non-Higgs backgrounds. We used them as input patterns for Background NN-training. (solid: $Z^0 H$, dotted: W^+W^- , dash-dotted: $Z^0 Z^0$).

B. 4-jet mode

Selection criteria of 4-jet events for reduction of backgrounds from e^+e^- collision are as following: (1) the visible energy is greater than 210 GeV, (2) $\cos\theta$ of thrust axis(called thrust angle) between -0.85 and 0.85 , (3) the Higgs mass between $103\text{ GeV}/c^2$ and $130\text{ GeV}/c^2$, (4) the Z^0 mass between $78\text{ GeV}/c^2$ and $102\text{ GeV}/c^2$, (5) the mass recoil to the Higgs jet pair be greater than $80\text{ GeV}/c^2$, (6) the number of particles in each jet of Higgs pair be greater than 5, and (7) the Ymax value greater than 0.01. Here we made forced 4-jet clustering, and the Higgs jet pair and Z^0 jet pair out of four jets were selected by χ^2 , which is defined as a squared sum of the differences of the reconstructed invariant mass of jet pair and the correct mass divided by its resolution of Higgs and Z^0 pair:

$$\begin{aligned} \chi^2 = & \left(\frac{M_{Z^0} - 91.2}{width} \right)^2 + \left(\frac{M_{recoilZ^0} - 91.2}{width} \right)^2 \\ & + \left(\frac{M_H - 120}{width} \right)^2 + \left(\frac{M_{recoilH} - 120}{width} \right)^2. \end{aligned}$$

From the 4 jets, only 2 jets which are assigned to Higgs are used for the vertex tagging, and we also required at least one successful secondary vertex reconstruction with MSPTM between $0.1\text{ GeV}/c^2$ and $7.0\text{ GeV}/c^2$ out of 2

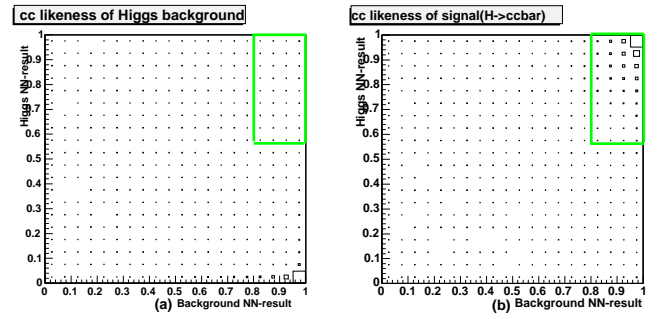


FIG. 4: 2D NN-result for $H \rightarrow c\bar{c}$ selection in 2-jet mode. From the left top, distributions in 2D NN-result of (a)Higgs backgrounds, (b) $H \rightarrow c\bar{c}$ signal event, and (c)non-Higgs backgrounds are shown. The signal region is seen at the right top.

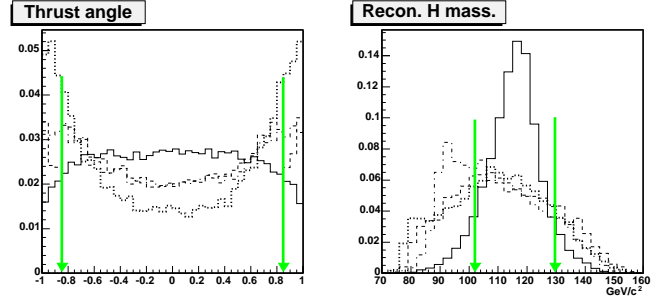


FIG. 5: Thrust angle and Higgs mass distributions. Cut points from the selection criteria are shown(solid: $Z^0 H$, dotted: W^+W^- , dash-dotted: $Z^0 Z^0$, dashed: $q\bar{q}$).

jets from Higgs. Higgs mass and thrust angle distributions of the signal and non-Higgs background events are shown in the Fig. 5. With the same procedure to the 2-jet study, we trained the NN with input patterns of normalized vertex information of ZVTOP program. The MSPTM and corrected secondary momentum distributions of the $c\bar{c}$ and other Higgs decays are seen in the Fig. 6. We also didn't use $H \rightarrow WW^*$ events due to its featureless patterns for more effective c quark selection in Higgs NN-training. In the Background NN-training, we additionally included thrust angle as a NN input pattern. As seen in the Fig. 7, the thrust angle shows clear separation between the signal and non-Higgs backgrounds. Similarly to the 2-jet study, we used both results of Higgs NN-training and Background NN-training, and the NN-

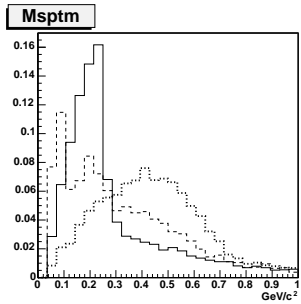


FIG. 6: MSPTM and the P_t corrected secondary momentum distributions of 4-jet samples for $H \rightarrow c\bar{c}$ distinction from other Higgs decays(solid: $H \rightarrow c\bar{c}$, dotted: $b\bar{b}$, dashed: gg).

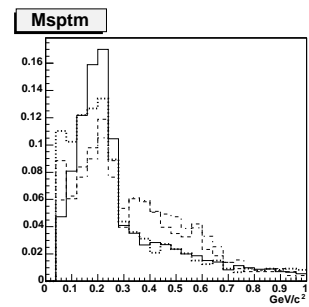
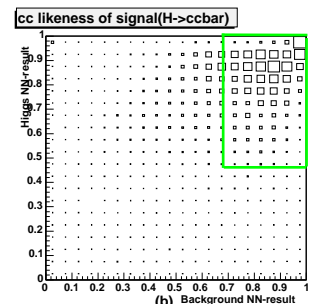
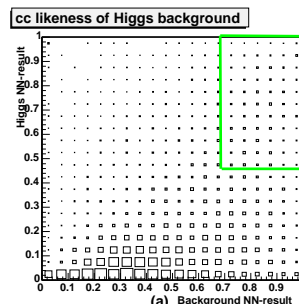
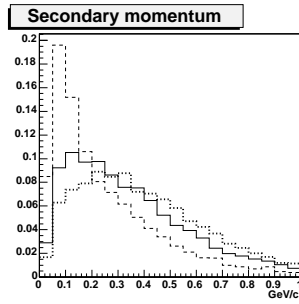
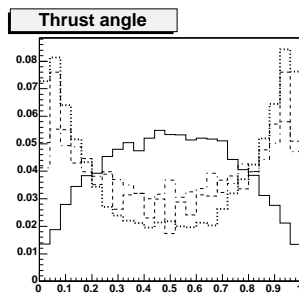


FIG. 7: MSPTM and thrust angle distributions for $H \rightarrow c\bar{c}$ distinction from non-Higgs backgrounds(solid: $Z^0 H$, dotted: $W^+ W^-$, dash-dotted: $Z^0 Z^0$, dashed: $q\bar{q}$).



result is shown in the Fig. 8 with signal box at the right top.

IV. DISCUSSION

The results of the 2-jet and 4-jet $c\bar{c}$ event selection are summarized in the Table II. As seen in the table, roughly 120 and 310 $H \rightarrow c\bar{c}$ events are selected in 2-jet and 4-jet modes, respectively, with a reasonable significance despite its small branching ratio of $H \rightarrow c\bar{c}$ and large backgrounds from non-Higgs processes and other Higgs decay modes.

In the $H \rightarrow c\bar{c}$ measurement in 2-jet mode, major backgrounds are those from $H \rightarrow b\bar{b}$ where b is misidentified as c and $W^+ W^-$ events which are reconstructed as 2-jet events due to imperfect detector acceptance. In the case of 4-jet mode, backgrounds from $W^+ W^-$ and $Z^0 Z^0$ processes are increased because two c jets are produced in the final state of these background processes. So we can use only kinematical information such as the invariant mass of jets for background discrimination. In addition to the c -jet contamination from backgrounds, there is another ambiguity in selecting Higgs jets out of four jets. Combining these effects, the significance in 4-jet mode is worse than 2-jet mode. The statistical error is estimated as 25.7% in the case of four CCD layers of the vertex

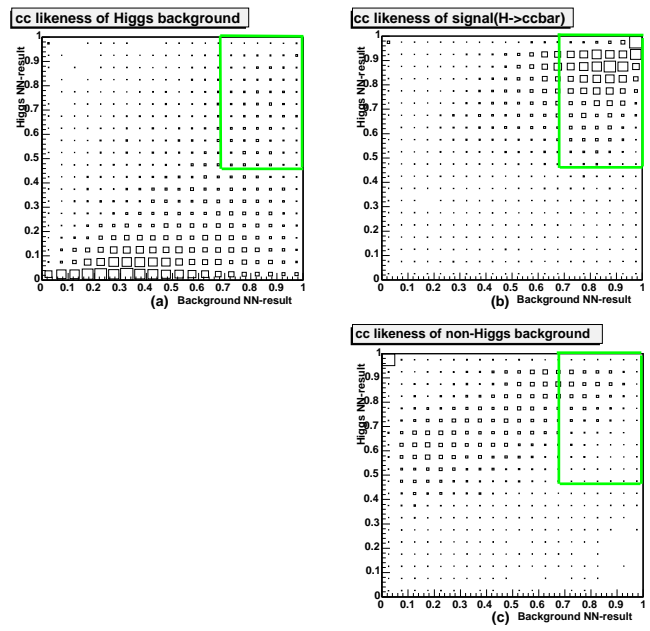


FIG. 8: 2D NN-result for $H \rightarrow c\bar{c}$ selection in the 4-jet Higgs events. From the left top, distributions in 2D NN-result of (a)Higgs backgrounds, (b) $H \rightarrow c\bar{c}$ signal event, and (c)non-Higgs backgrounds are shown. The signal region is seen at the right top.

detector with combination of both modes.

When an additional CCD layer of the vertex detector is included near the interaction point, the impact parameter resolution for low momentum track is improved since the lever arm for track extrapolation to the interaction point is reduced. Thus we can reconstruct secondary vertices much closer to the interaction points. As a result, backgrounds in the event selection are reduced especially in 2-jet mode thanks to the better separation of b jet and c jet. Improvements in 4-jet selection is not decisive, suffering ambiguities in Higgs jet selections. Combining 2-jet and 4-jet, about 20% improvement(relative) in background reduction is obtained compared to the four CCD layers of the vertex detector case.

These results are consistent with the study performed by Oregon group [12] but significantly worse than the results obtained by TESLA Higgs group [13].

V. SUMMARY

In this study, we have focused on the $H \rightarrow c\bar{c}$ measurements in 2-jet and 4-jet modes in the case of the Higgs mass of 120 GeV/c^2 with the center-of-mass energy of 250 GeV at the future $e^+ e^-$ linear collider. For the detector configuration, we considered the JLC detector equipped with a four CCD layers of the vertex detector and those with additional fifth layer of the vertex detector. In the study, the topological vertex finding algorithm was used for tagging c quark jet and the neural network was used

Number of CCD layers	4 CCD layers		5 CCD layers	
Decay mode \ Events	2-jet	4-jet	2-jet	4-jet
$H \rightarrow c\bar{c}$	122.7(17.6)	306.3(12.6)	112.7(16.2)	316.8(13.0)
$H \rightarrow b\bar{b}$	641.8(4.2)	2686.7(5.0)	231.2(1.5)	1807.2(3.4)
$H \rightarrow gg$	28.1(1.8)	217.6(3.9)	8.9(0.6)	143.4(2.6)
$H \rightarrow WW^*$	23.6(0.8)	226.7(2.1)	10.1(0.3)	178.0(1.7)
$e^+e^- \rightarrow W^+W^-$	640(0.008)	9790(0.130)	330(0.004)	8530(0.110)
$e^+e^- \rightarrow Z^{\circ}Z^{\circ}$	100(0.016)	1710(0.274)	30(0.004)	1305(0.209)
$e^+e^- \rightarrow q\bar{q}$	20(<0.001)	1730(0.007)	5(<0.001)	1345(0.006)
S/N	0.0843	0.0187	0.1832	0.0238
$S/\sqrt{S+N}$	3.09	2.37	4.17	2.71
Statistical Error		25.7 %		20.1 %

TABLE II: The number of c quark tagged events, efficiency (percentage in parenthesis), and significance(last three rows) of $H \rightarrow c\bar{c}$ measurements for two different vertex detector parameters. We used 100 fb^{-1} in this analysis and scaled up to 500 fb^{-1} in this table.

to optimize the $H \rightarrow c\bar{c}$ selection.

We obtained 25.7% for the measurement of $H \rightarrow c\bar{c}$ with the data of 500 fb^{-1} at the center-of-mass energy of 250 GeV in the case of four layer vertex detectors. Statistical error is improved to 20.1% if an additional CCD layer of vertex detector is included near the interaction point.

We would like to thank the members of ACFA Joint Linear Collider Physics and Detector Working group [14]

for valuable discussions during the course of the analysis. We also thank Dr. David Jackson for allowing us to use his ZVTOP program. Akiya Miyamoto is partially supported by Japan-Europe Research Cooperative Program and Hwanbae Park is supported by Korea Research Foundation Grant(KRF-2002-003-C00035). JooSang Kang and Geum Bong Yu are supported by Korea University Grant.

[1] S. L. Glashow, Nucl. Phys. **22**, 579 (1961) ; S. Weinberg, Phys. Rev. Lett. **19**, 1264 (1967) ; A. Salam, in *Elementary Particle Theory*.

[2] The LEP Collaborations, the LEP Electroweak Working Group, and the SLAC heavy flavour group, LEPEWWG/2003-01 (2003).

[3] H. P. Nilles and M. Nusbaumer, Phys. Lett. **B 145**, 73 (1984).

[4] J. Kamoshita, Y. Okada, and M. Tanaka, Phys. Lett. **B 328**, 67 (1994) ; T. Moroi and Y. Okada, Phys. Lett. **B 295**, 73 (1992).

[5] “Report on the international detector R & D”, See “<http://blueox.uoregon.edu/~lc/randd.html>”.

[6] T. Sjostrand, Comput. Phys. Commun. **82**, 74 (1994).

[7] A. Djouadi, J. Kalinowski, and M. Spira, Comput. Phys. Commun. **108**, 56 (1998).

[8] JLC Study Framework, See “<http://www-jlc.kek.jp/subg/offl/jsf>”.

[9] K. Abe *et al.*, KEK Report 2001-11 (2001).

[10] D. J. Jackson, Nucl. Instrum. Meth. **A 388**, 247 (1997).

[11] C. Peterson, T. Rognvaldsson, and L. Lonnblad, Comput. Phys. Commun. **81**, 185 (1994).

[12] J. Brau *et al.*, “Flavor Tagging and the Higgs Branching Ratio measurement at the Linear Collider”, in the proceedings of International Workshop on Linear e^+e^- Colliders 2002, ed. J. S. Kang and S. K. Oh, Jeju, Korea, 2002, p.487.

[13] J-C. Brént, The direct method to measure the Higgs branching ratios at the future e^+e^- linear collider, LLR 02-002, See “<http://www.desy.de/~desch/higgs>”.

[14] See “<http://acfahep.kek.jp>”.